

A Mesoproterozoic paleomagnetic pole from the Yangzhuang Formation, North China and its tectonics implications

Junling Pei^a, Zhenyu Yang^{b,*}, Yue Zhao^a

^a Key Laboratory of Crust Deformation and Processes, Institute of Geomechanics, CAGS, Beijing, China

^b Department of Earth Sciences, Nanjing University, Nanjing, China

Received 22 August 2005; received in revised form 12 May 2006; accepted 6 June 2006

Abstract

A new paleomagnetic study has been carried out on Mesoproterozoic sediments in the Jixian area, North China. Detailed stepwise thermal demagnetization allows us to isolate three components from 141 oriented drill-core samples (14 sites). A low-temperature component (component A) identified from most of samples falls close to the present local earth field direction. A middle-temperature component (component B) is found only in 21 samples from four sites. The component B directions (after bedding correction) yield a paleopole position at 336.0°E, 10.2°N with $A_{95} = 17.1^\circ$, which is close to the Lower Cambrian pole of the North China Block. Characteristic remanent directions with dual polarities obtained from high-temperature (component C) pass fold test. The directions yield a pole position at 190.4°E, 2.4°N with $A_{95} = 11.9^\circ$. This result indicates that the North China Block was located in low latitude at ca. 1.35 Ga. Recently, several studies suggested that Laurentia, Baltica and Siberia were also situated at low latitudes from well dated paleopoles between ca. 1.5 and 1.25 Ga. This would imply that the North China Block, Laurentia and Baltica might drift together or close in the Mesoproterozoic.

© 2006 Elsevier B.V. All rights reserved.

Keywords: The North China Block; Paleomagnetic; Mesoproterozoic

1. Introduction

The existence of a pre-Rodinia supercontinent has been profoundly discussed during last decade (Hoffman, 1989; Rogers, 1996; Condie, 2002; Rogers and Santosh, 2002; Wilde et al., 2002; Zhao et al., 2004). Rogers and Santosh (2002) named this supercontinent as Columbia that lived from ca. 1.8 to 1.5 Ga, and proposed a configuration based on evidences of rifting and orogenic activities. Zhao et al. (2002) extended this hypothesis to most cratonic blocks and suggested a new configuration

of Columbia supercontinent based on the available geological reconstructions of 2.1–1.8 Ga orogens and related Archean cratonic blocks. Two years later, Zhao et al. (2004) gave a detailed review in the assembly, growth and breakup of such a pre-Rodinia supercontinent, and concluded that the assembly of Columbia supercontinent finished at ca. 1.8 Ga, after a long-lived growth, its final breakup occurred at about 1.3–1.2 Ga. As the only quantitative method for testing the proposed configuration, paleomagnetism was widely used to infer the existence of pre-Rodinia supercontinent (e.g., Buchan et al., 2000; Meert, 2002). Most recently, on the basis of high quality paleomagnetic data and geochronological/geological information, Pesonen et al. (2003) proposed a “Hudsonland” supercontinent during the Paleo-Mesoproterozoic (ca. 1.8 Ga to 1.5–1.25 Ga). Unfortunately, due to the

* Corresponding author at: Department of Earth Sciences, Nanjing University, 22, Hankou Road, Nanjing 210093, China.

Tel.: +86 25 83597065; fax: +86 25 83686016.

E-mail address: paleo_mag@yahoo.com.cn (Z. Yang).

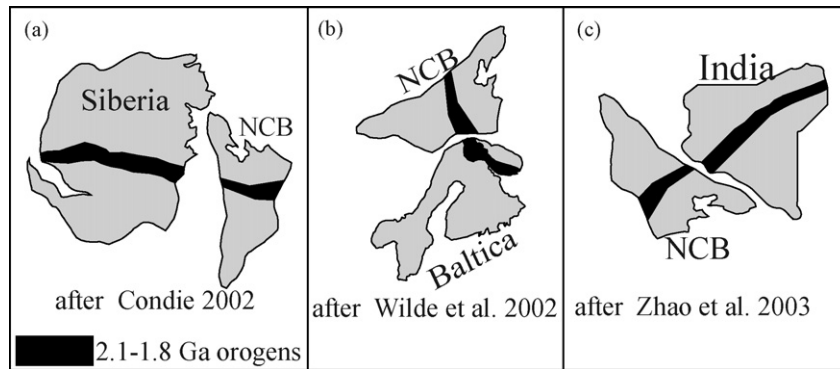


Fig. 1. Examples of Proterozoic connections between (a) North China Block and Siberia, (b) Baltica and (c) India from the literature.

lack of reliable paleomagnetic data, the position of the North China Block is clearly not well defined.

Several models concerned the paleo-position of the North China Block during the Paleo-Mesoproterozoic were proposed based on the geological data, e.g., it was adjacent to Siberia (Fig. 1a, Li et al., 1996a, 1996b; Condie, 2002), or next to the western margin of Baltica (Fig. 1b, Wilde et al., 2002), or close to southern India during the Archean to Paleoproterozoic (Fig. 1c, Zhao et al., 2003), or connected with Laurentia between 1200 and 700 Ma (Zhang et al., 2006). In this study, we report a new Mesoproterozoic paleomagnetic result from the Jixian area of the North China Block, and discuss the paleo-position of the North China Block at ca. 1.35 Ga.

2. Geological setting and paleomagnetic sampling

Zhao et al. (2005a, 2005b) suggested a ca. 1.85 Ga collision model for the final consolidation of the North China Block by amalgamation of the Eastern Block and the Western Block along a central orogenic belt (Fig. 2). It is still a debate for the collision time, e.g., at ca. 1.85 Ga (Guan et al., 2002; Kröner et al., 2005), or ca. 2.5 Ga (Kusky et al., 2001; Zhai and Liu, 2003).

It is a remarkable feature that a typical aulacogenic sedimental record with a total of thickness of 9193 m is preserved in an intracratonic rift basin named Yanshan-Taihangshan aulacogen in the central North China Block (Lu et al., 2002). The most complete stratigraphic sequence is well exposed in Jixian area where the tectono-sedimentary setting is simple. The sequence is a type section of Proterozoic strata in China known as the Jixian section (Lee, 1939; Chen et al., 1981). In the last decade, major advancements of the Jixian section have been achieved on the sedimentology, paleontology and geochemistry (Lu and Li, 1991; Li et al.,

1995, 2003). The Jixian section can be divided into three systems, in ascending order: the Changcheng system (1.8–1.4 Ga), the Jixian system (1.4–1.0 Ga) and the Qingbaikou system (1.0–0.8 Ga) (Fig. 3). Two layers volcanic rocks were developed in the Tuanshanzi and Dahongyu Formations of the Changcheng system. They yielded single-zircon U-Pb ages of 1683 ± 67 Ma and 1625 ± 6 Ma, respectively (Lu and Li, 1991; Li et al., 1995). Several ^{40}Ar - ^{39}Ar ages have been obtained from cherts within dolostone of the Gaoyuzhuang, Yangzhuang and Wumishan Formations, and glauconites within the Hongshuizhuang, Tieling and Jing'eryu Formations (Fig. 3; Wang et al., 1995; Li et al., 1996a, 1996b).

We sampled the Mesoproterozoic rocks along a road from Beijing to Jixian city (Fig. 2; 40.2°N , 117.3°E). The Yangzhuang Formation mainly consists of predominantly marine alternating white and red sandy dolostone intercalated with thin-bedded siliceous rocks including cherts and depositional quartz with textures of pebble in its lower part, purple thick-bedded and minor grayish-white muddy dolostone in the middle part and white-red dolostone interbedded with chert nodules in the upper part (BGMRT, 1989). The Yangzhuang Formation is conformably or disconformably underlain by the Gaoyuzhuang Formation that contains the macroalgal fossils, *Grypania spiralis*, *G. sangshuanensis*, *G. linearis*, *G. buccinata* and is conformably overlain by the Wumishan Formation that yields abundance of stromatolites, mainly including *Pseudogymnosolen mopanyuensis*, *Coalesca regularis*, *Comophyton litunm* and *Microcollenia bellala* (BGMRT, 1989).

A total of 141 samples from 14 sites within the middle of the Yangzhuang Formation were collected using a water-cooled portable drill and orientated using a magnetic compass. Six sites JX10 to JX15 and two sites JX16 and JX17 were sampled from both flanks of the

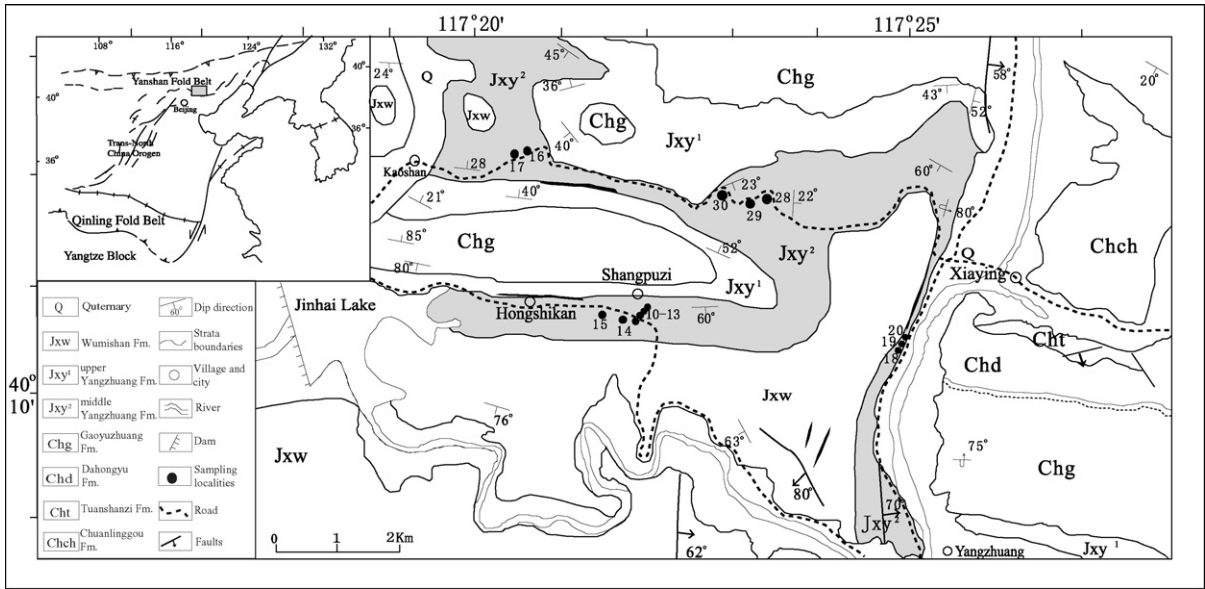


Fig. 2. Geological sketch map of the sampling area in the northern part of Jixian city in the North China Block. Inset map shows the tectonic framework of North China and the location of the study area. Locations of our sites (circles) are shown in the area.

Era	System	Formation Thickness	Lithology column	Age and reference	
Neoproterozoic	Qingbaikou	Jing'eryu 203m	[Lithology pattern]	816 ± 9.1 Ma, Glauconite, $^{40}\text{Ar}-^{39}\text{Ar}$, Li Mingrong et al., 1996	
		Xiamaling 168m	[Lithology pattern]	880 ± 8.5 Ma, Glauconite, $^{40}\text{Ar}-^{39}\text{Ar}$, Li Mingrong et al., 1996	
Mesoproterozoic	Jixian	Tieling 330m	[Lithology pattern]	1082 ± 13 Ma, Glauconite, $^{40}\text{Ar}-^{39}\text{Ar}$, Li Mingrong et al., 1996	
		Hongshuizhuang 131m	[Lithology pattern]	1175 ± 10 Ma, Glauconite, $^{40}\text{Ar}-^{39}\text{Ar}$, Li Mingrong et al., 1996	
		Wumishan 3336m	[Lithology pattern]	1207 ± 10 Ma, Cherts, $^{40}\text{Ar}-^{39}\text{Ar}$, Wang Songshan et al., 1995	
		Yangzhuang 707m	upper yz' 340m	[Lithology pattern]	1317 ± 22 Ma, Cherts, $^{40}\text{Ar}-^{39}\text{Ar}$, Wang Songshan et al., 1995
			middle yz' 160m	[Lithology pattern]	★ suggested age 1.35Ga
	lower yz' 207m	[Lithology pattern]	1380 ± 24 Ma, Cherts, $^{40}\text{Ar}-^{39}\text{Ar}$, Wang Songshan et al., 1995		
	Changcheng	Gooyuzhuang 1569m	[Lithology pattern]	ca.1434Ma, Galena, Pb - Pb, Chen et al., 1981	
		Dahongyu 480m	[Lithology pattern]	1625 ± 6 Ma, Zircon, U-Pb, Lu Songnian et al., 1991	
		Tuanshanzi 518m	[Lithology pattern]	1683 ± 67 Ma, Zircon, U-Pb, Li Huaikun et al., 1995	
		Chuanlinggou 889m	[Lithology pattern]		
Changzhougou 854m		[Lithology pattern]			

[Lithology pattern]	[Lithology pattern]	[Lithology pattern]	[Lithology pattern]	[Lithology pattern]	[Lithology pattern]	[Lithology pattern]
Volcanics	Dolostone	Limestone	Shale	Sandstone	Sampling section	

Fig. 3. Generalized stratigraphy for Jixian section in the North China Block, showing isotopic ages from earlier studies.

Hongshikan fold, respectively (Fig. 2), and three sites JX18, JX19 and JX20 closed to a fault where the bed is inversed and three sites JX28, JX29 and JX30 from northeast limb of the fold where the strikes and dips changed greatly were collected. The Hongshikan fold was formed at the Late Triassic based on the newest SHRIMP U-Pb ages of volcanic sills in the sampling area (Zhao et al., 2005a, 2005b).

In the laboratory, one or two 2.2-cm long cylindrical specimens were sliced from each sample with a diamond saw for further rock magnetic and paleomagnetic measurements.

3. Paleomagnetic results

3.1. Treatments

All samples were subsequently subjected to progressive thermal demagnetization up to 680 or 690 °C in 16–20 steps using an ASC-Scientific TD-48 thermal demagnetizer with an interval residual field lower than 10 nT. The natural remanent magnetization (NRM) were measured on a 2 G-755 cryogenic magnetometer inside a set of large Helmholtz coils that reduce the ambient geomagnetic field to around 300 nT in the paleomagnetic Laboratory of the Institute of Geomechanics in Beijing. Results were analyzed by principal component analysis (Kirschvink, 1980) and Fisher statistics (1953) or the McFadden and McElhinny method (1988).

In order to determine the magnetic carriers within the samples, both acquisition of isothermal remanent magnetization (IRM) and three-axis thermal demagnetization of IRMs (Lowrie, 1990) were conducted in the laboratory. Fields of 2.4, 0.4 and 0.12 T were applied successively along Z, Y and X axes of the specimens, respectively. Then stepwise thermal demagnetization up to 685 °C is performed. IRM experiments were measured using the IM-10 impulse magnetizer and the DSM-2 magnetometer.

3.2. Rock magnetic results

Rock magnetic experiments are designed to identify the magnetic minerals within the rocks. Acquisition and opposite field demagnetization behavior of IRM are observed for selected specimens from 14 sites. The IRM curves show that no saturation is achieved after applying the fields up to 2.4 T and a quasi-saturation (>80%) behavior at about 1.1 T (Fig. 4a, c, e, g). Combining remanent coercivity ($H_{cr} > 500$ mT) deduced from back-demagnetization with three-component IRM thermal demagnetization, the presence of high-coercivity

hematite minerals in these samples is evidenced. The results exhibit a wide range coercivity fractions carried by hematite (Fig. 4b, d, f, h). The soft component is unblocked around 580 °C (Fig. 4d, f, h), suggesting the presence of a few magnetite. These experiments indicate that hematite is the main magnetic carrier in dolostone of the Yangzhuang Formation. Magnetite probably exists in part of the rocks.

3.3. Magnetic component analysis

One hundred and forty-two samples (14 sites) were measured using thermal demagnetization with temperature intervals ranging from 80 °C at the lower temperature to 10 °C or 5 °C at the high temperature. Three NRM components are recognized in the samples.

The component A can be identified between NRM and 240 °C from most of the samples, which has a northerly declination and a steep positive inclination in situ coordinates (Fig. 5). The site-mean direction (Dec = 2.0°, Inc = 63.1°, $\alpha_{95} = 6.0^\circ$, $N = 137$ samples) before bedding correction is indistinguishable from the present dipole field which is Inc = 59.4° (Fig. 6a, b and Table 1). The decrease of the precision parameters (k) from 44.2 to 2.0 after tilt correction shows that the component A has been acquired after folding and is probably a viscous remanent magnetization (Fig. 6c).

A different component B is separated between 300 and 530–580 °C in 21 samples from four sites (Fig. 5a, b). The average site-mean direction is $D = 241.8^\circ$, $I = -49.5^\circ$, $\alpha_{95} = 15.0^\circ$, and $D = 315.8^\circ$, $I = -47.0^\circ$, $\alpha_{95} = 16.5^\circ$ before and after tilt corrections, respectively (Fig. 6d, e and Table 1). The precision parameters (k) of site-mean directions before and after bedding corrections are not significantly change due to the monoclinical nature of sampling sites ($k_s/k_g = 38.7/31.8$).

Except few samples demonstrate only a component A (Fig. 5f), a higher temperature component C of both reversed and normal polarities is isolated up to 680 or 690 °C from most of samples (Fig. 5, Table 1), which decays linearly to the origin revealed from two-third of samples. Remanent directions after 660 °C become erratic in about one-third samples, however, a well-defined great circle paths are usually shown on the stereographic plot (Fig. 5g, j). The site-mean direction is then computed using the intersection of sector-constrained great circles combined with directly observed directions by the statistical method developed by McFadden and McElhinny (1988) (Fig. 7). Most sites are of mixed polarity with the exception of site JX10, JX14 and JX30 of normal polarity and site JX29 with reversal polarity.

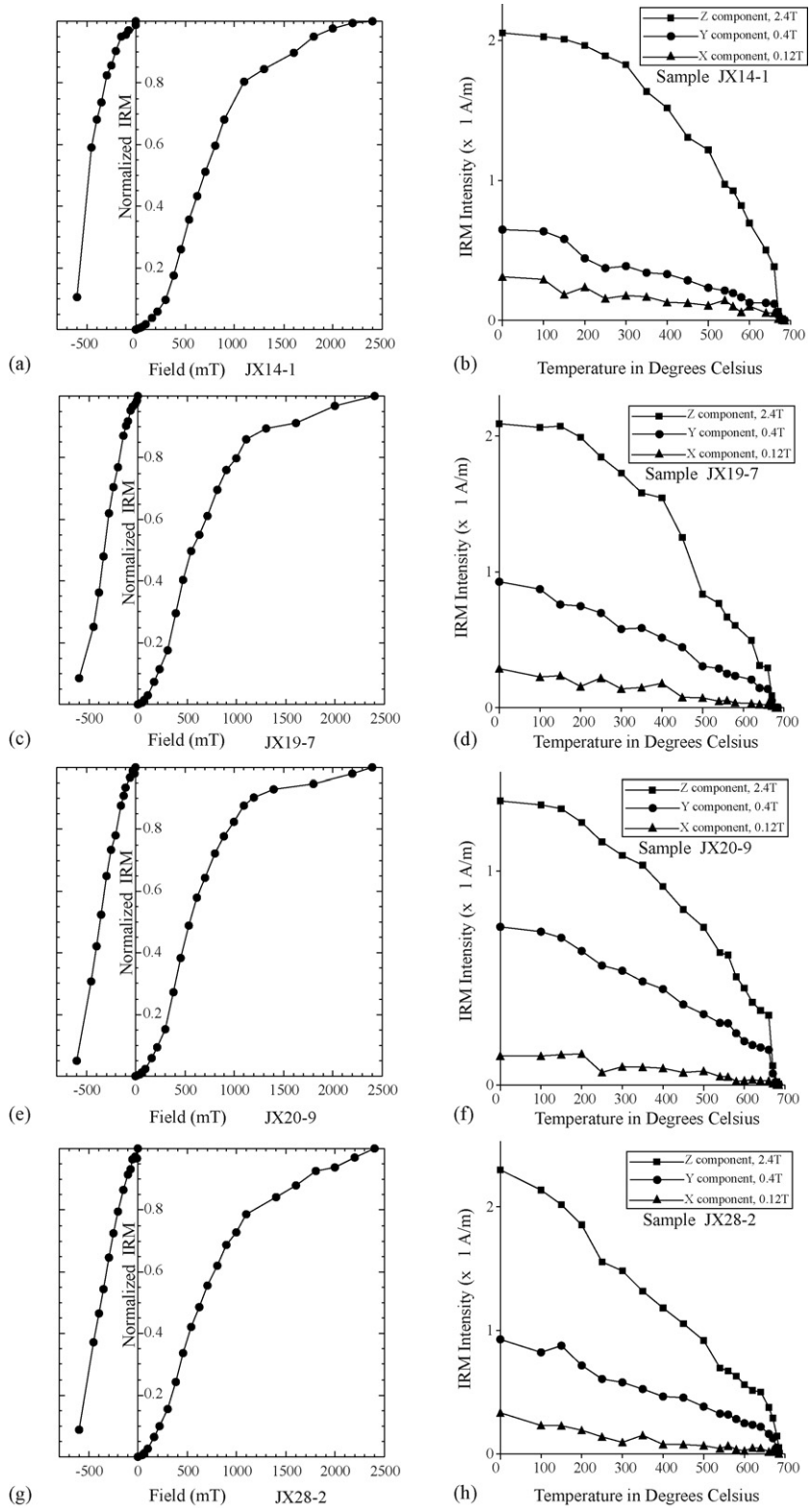


Fig. 4. Normalized isothermal remanent magnetization (IRM) and opposite field demagnetization acquisition curves of representative samples (a, c, e, g); three-axis IRM thermal demagnetization showing unblocking temperatures around 680 °C (b, d, f, h).

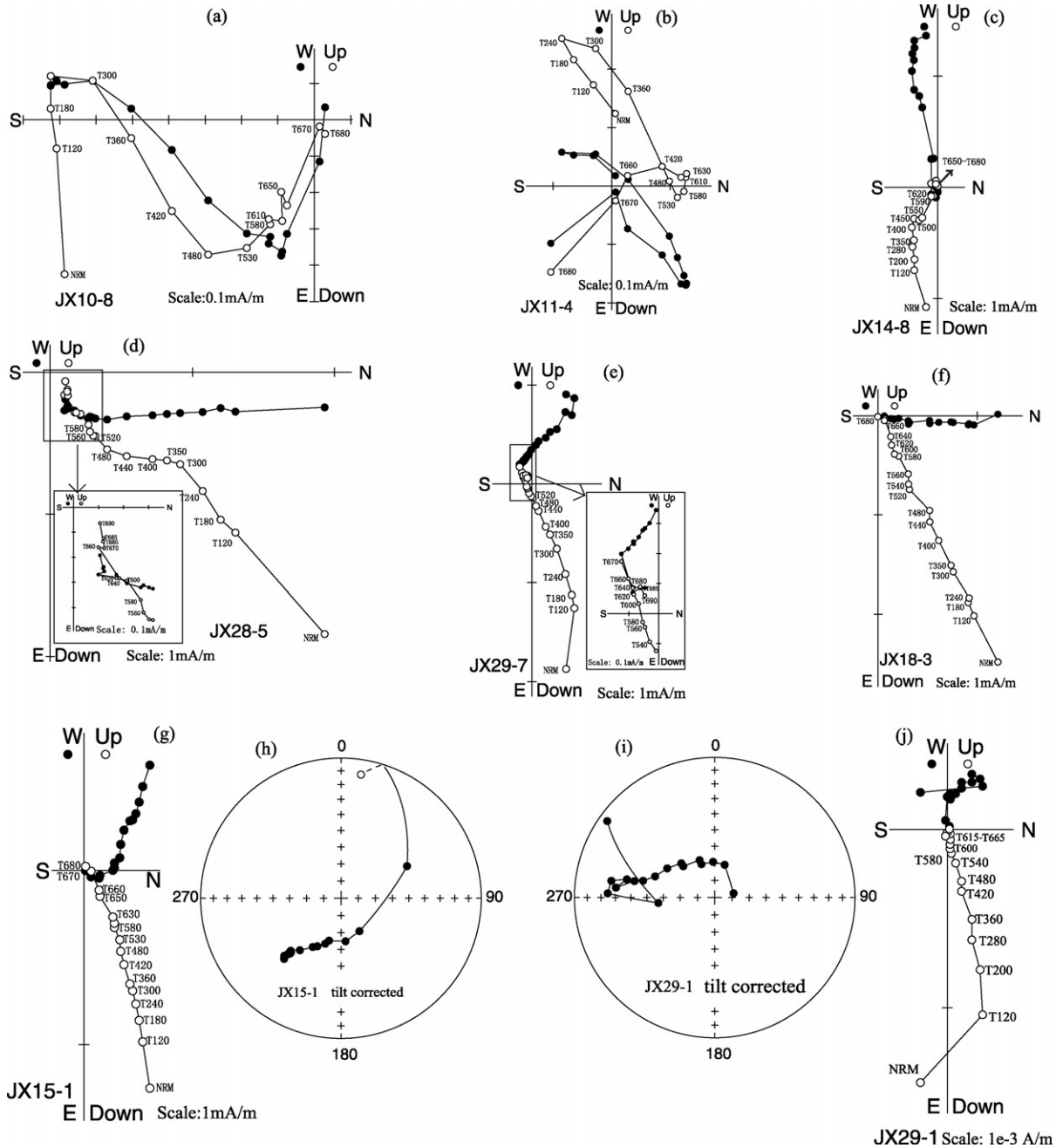


Fig. 5. (a–f) Selected Zijderveld diagrams of thermal demagnetizations of NRM showing three components in situ coordinates (a, b), two components (c, d, e) and one component (f). (g, j) Orthogonal vector projection of NRM thermal demagnetization showing erratic directional changes after heating to 600–670 °C in situ coordinates, and (h, i) stereographic projections of the change in NRM directions along remagnetization great circles after tilt corrections. Solid (open) symbols refer to the projection on the horizontal (vertical) plane. 200 = 200 °C. Stereoplot with solid (open) symbols in the lower (upper) hemisphere.

The tilt correction greatly improves the clustering of site-mean directions for component C (Fig. 6g, h). The ratio of precision parameters is reached maximum at 100% unfolding (Fig. 6f). The average site-mean direction is $D=80.2^\circ$, $I=20.3^\circ$, $\alpha_{95}=24.3^\circ$

before, and $D=99.3^\circ$, $I=27.2^\circ$ and $\alpha_{95}=14.8^\circ$ ($ks/kg=10.5/4.5$) after tilt corrections (Table 1, Fig. 6g, h). The fold test is positive at the 95% probability level according to the both fold tests of McElhinny (1964) and the Watson and Enkin (1993). The latter

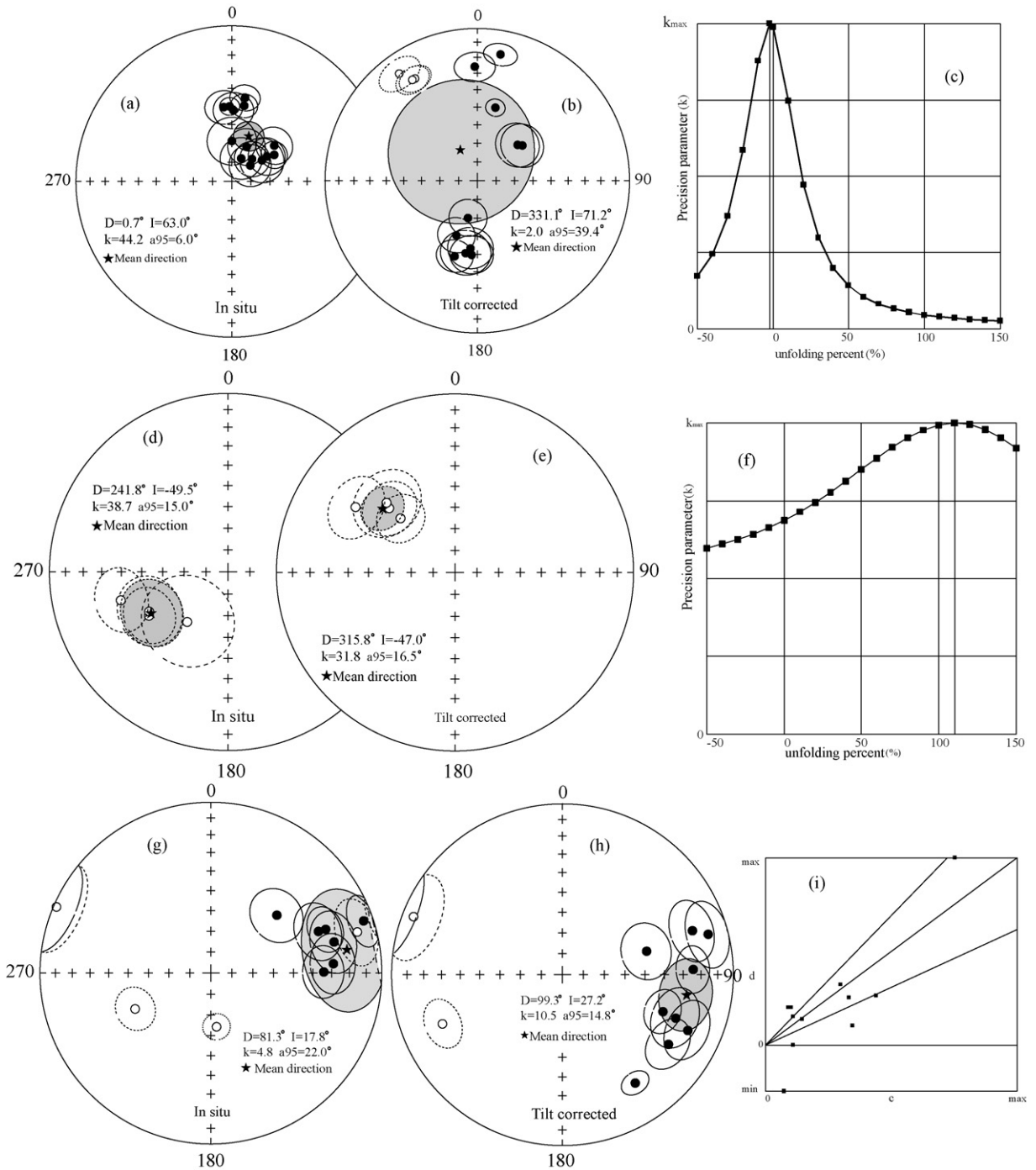


Fig. 6. Equal-area stereographic projections of the component A site-mean in (a) before and (b) after tilt corrections. (d, e) Site-mean directions of the component B. (g, h) Site-mean directions of the component C. The change of the precision parameter (k) of the component A (c) and the component C (f) during unfolding analysis. (i) The D-C tilt test (Enkin, 2003) plot shows a positive test. Lower (upper) hemisphere directions are marked with solid (open) symbols.

Table 1

Site-mean directions and corresponding poles from Mesoproterozoic Yangzhuang Formation in Jixian area (117.3°E, 40.2°N), North China

Site	Strike/dip	n/N_0	N/R	Dg	Ig	Ds	Is	k	α_{95}	$P_{lat.}$	$P_{long.}$
Lower temperature component A											
JX10	189/53	9/10	9/0	22.5	77.0	184.4	49.5	23.2	10.9		
JX 11	186/58	10/10	10/0	1.4	52.3	194.1	69.4	24.2	10.0		
JX 12	186/59	10/10	10/0	349.9	60.7	201.0	58.4	25.9	9.7		
JX 13	182/56	9/10	9/0	355.1	70.7	185.8	53.1	20.6	11.6		
JX 14	186/61	9/10	9/0	0.3	68.8	189.2	50.1	17.5	12.7		
JX 15	187/57	10/10	10/0	342.2	74.2	196.7	47.0	28.6	9.2		
JX 16	10/25	13/15	13/0	353.9	50.3	358.7	26.0	20.9	9.3		
JX 17	14/28	9/9	9/0	9.1	44.7	10.4	16.8	51.0	7.3		
JX 18	124/79	10/10	10/0	23.3	70.3	323.9	-14.0	33.8	9.7		
JX 19	126/83	10/10	10/0	358.0	63.0	328.6	-22.5	41.3	7.6		
JX 20	126/83	10/10	10/0	356.9	64.4	327.2	-22.3	37.5	8.0		
JX 28	92/13	10/10	10/0	358.4	50.1	13.9	49.1	99.8	4.9		
JX 29	66/22	10/10	10/0	349.3	77.2	48.4	61.0	20.3	11.0		
JX 30	152/23	8/8	8/0	22.6	52.7	52.0	59.2	17.0	13.8		
Mean	-	14	-	2.0	63.1	-	-	44.2	6.0		
				-	-	331.1	71.2	2.0	39.4		
Middle temperature component B											
JX10	189/53	5/10	0/5	235.4	-49.6	314.8	-54.6	49.2	11.0		
JX11	186/58	7/10	0/7	243.3	-49.1	315.5	-44.5	16.4	15.4		
JX12	186/59	6/10	0/6	255.2	-37.9	303.3	-33.8	25.8	13.4		
JX15	187/57	3/10	0/3	241.0	-48.1	314.3	-47.3	101.1	12.3		
Mean	-	4	-	241.8	-49.5	-	-	38.7	15.0		
				-	-	315.8	-47.0	31.8	16.5	10.2	336.0
									17.1		
Higher temperature component C											
JX10	189/53	8/10	8/0	89.4	34.3	123.3	26.7	26.3	11.1	-14.4	174.1
JX 11	186/58	10/10	8/2	71.1	6.2	87.7	24.4	26.7	9.5	9.9	198.9
JX 12	186/59	10/10	9/1	75.8	26.6	111.0	29.7	15.6	12.8	-4.9	181.6
JX 13	182/56	10/10	8/2	85.6	28.9	114.0	20.8	16.6	12.2	-10.6	183.3
JX 14	186/61	8/9	8/0	74.3	-12.0	74.5	12.5	20.1	12.7	15.9	212.5
JX 15	187/57	9/10	8/1	69.1	28.9	110.2	37.4	35.5	9.6	-0.9	178.6
JX16*	12/26	7/24	2/5	293.2	-1.9	291.3	-7.2	19.1	16.1	13.7	10.4
JX18*	126/83	10/30	7/3	174.0	-64.2	146.1	24.6	82.8	6.0	-28.3	155.4
JX 28	92/13	9/10	8/1	68.8	33.0	71.3	20.8	18.4	12.4	21.2	211.0
JX 29	66/22	9/10	0/9	244.7	-49.4	247.7	-25.1	32.5	9.9	-25.4	31.4
JX 30	152/23	4/8	4/0	48.7	47.4	74.4	47.6	98.0	12.7	29.4	193.0
Mean	-	11	-	80.2	20.3	-	-	4.5	24.3		
				-	-	99.3	27.2	10.5	14.8	2.4	190.4
									11.9		

Abbreviations: JX16* = JX16 and JX17; JX18* = JX18, JX19 and JX20; Strike/dip = strike azimuth and dip of bed; n/N_0 = number of samples used to calculate mean/total samples demagnetized; N/R = number of samples exhibiting normal/reversal polarity; Dg/Ig (Ds/Is) = declination and inclination in situ (after tilt correction); $P_{lat.}/P_{long.}$ = north latitude/east longitude of virtual geomagnetic pole; k = the precision parameter; α_{95} = the radius that the mean direction (pole) lies within 95% confidence. Fold test for the higher temperature component C, (1) McElhinny's (1964) method, $ks/kg = 10.5/4.5 = 2.33 > F(2*(n2 - 1), 2*(n1 - 1)) = 2.12$ at 95% confidence level, (2) Watson and Enkin (1993) fold test gives a maximum grouping of directions at 101.6% unfolding (with uncertainties ranging from 96.6 to 106.5%), and (3) direction-correction tilt test (Enkin, 2003) with the optimal clustering is at $99.9 \pm 38.3\%$ untilting; McFadden and McElhinny's (1990) reversal test, angle between the mean directions $\gamma = 31.4^\circ < \gamma_{critic} = 50.3^\circ$ indicates it is considered to be positive but is to be classified as 'INDETERMINATE' for $\gamma_{critic} = 50.3^\circ > 20^\circ$.

gives a maximum grouping of directions at 101.6% unfolding (with uncertainties ranging from 96.6 to 106.5%). The result is similar, with positive fold test using the direction-correction tilt test (Enkin, 2003) that the optimal clustering is at $99.9 \pm 38.3\%$

untilting (Fig. 6i). The McFadden and McElhinny's (1990) reversal test of the component C directions is inconclusive with angle between the mean directions $\gamma = 31.4^\circ < \gamma_{critic} = 50.3^\circ$ ('INDETERMINATE' class for $\gamma_{critic} = 50.3^\circ > 20^\circ$). The component C with dual

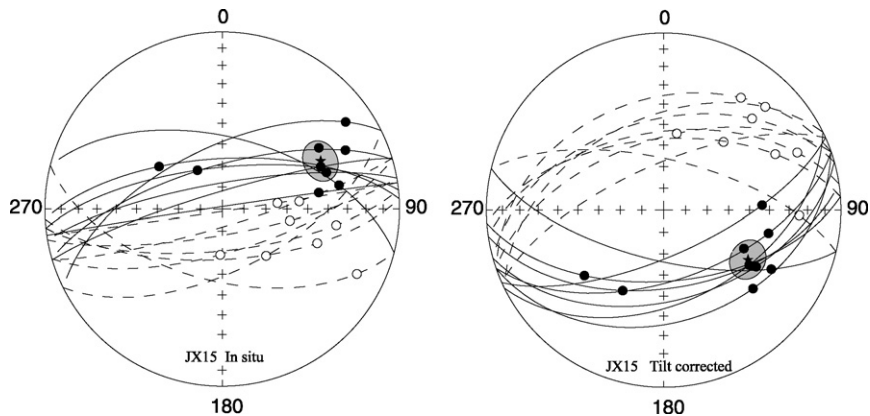


Fig. 7. The site-mean direction (star) for the site JX15 before and after tilt corrections calculated from the intersection of the great circles with limiting sector constraints and directly observed components. Solid (open) symbols represent directions plotted on the lower (upper) hemisphere.

polarity and positive fold test most likely represents the primary remanence of the Meso-Proterozoic sediments.

4. Discussion

It is important for a paleomagnetic pole that includes reliable dating used to analyze Precambrian plate tectonics (Buchan et al., 2000). Amounts of isotopic dates from U-Pb, ^{40}Ar - ^{39}Ar and Pb-Pb methods have been used to date most of records in Jixian section (Fig. 3). The age of the Yangzhuang Formation is constrained by ^{40}Ar - ^{39}Ar ages from cherts within dolostone in the boundary of the Gaoyuzhuang and Yangzhuang Formations and the top of the Yangzhuang Formation, which have been dated at 1380 ± 24 Ma and 1317 ± 22 Ma, respectively (Wang et al., 1995). Therefore, according to the age constraints mentioned above, an age of 1.35 Ga can be reasonably assigned to the paleomagnetic pole obtained from the middle part of Yangzhuang Formation sediments.

According to magnetic mineralogical studies, hematite with both high-coercivity and high-unblocking temperature is the major remanent carrier in measured samples. Because sampling areas locate in a simple fold belt and no major metamorphic event is known to have affected the sampling region. The high-temperature characteristic remanent magnetization (ChRM) passes positive fold test and with dual polarity, implying that the component C is acquired before strata folding during a long time instead of in a short remagnetization event. In addition, corresponding paleomagnetic pole at 190.4°E , 2.4°N ($A_{95} = 11.9^\circ$) is completely different from the Phanerozoic poles (Yang et al., 1998) and a series of late Mesoproterozoic to Neoproterozoic poles including the ca. 1270 Ma Yunmengshan formation pole (87.0°E , 60.6°S with $A_{95} = 3.7^\circ$), ca. 1200 Ma

Baicaoping formation pole (143.8°E , -43.0°A with $S_{95} = 11.1^\circ$), ca. 950 Ma Cuizhuang formation pole (44.8°E , -41.0°S with $A_{95} = 11.3^\circ$) and ca. 650 Ma Dongjia formation pole (97.4°E , 60.3°S with $A_{95} = 4.3^\circ$, $dm = 8.5^\circ$) (Zhang et al., 2006).

The paleomagnetic pole calculated from the site-mean directions of the component B after tilt correction is at 336.0°E , 10.2°N ($A_{95} = 17.1^\circ$), which appears to be statistically insignificant to the early Cambrian pole reported from the North China Block at the 95% confidence level (Huang et al., 1999). The component B represents likely an Early Cambrian overprint.

Therefore, the component C, prior to Early Cambrian overprint component B, with positive fold test and dual polarities, differs significantly from the post-Mesoproterozoic poles of the North China Block, represents probably the original remanent direction.

Paleomagnetic data have been published on the Paleo-Mesoproterozoic rocks in Jixian section of the North China Block (Zhang and Zhang, 1985; Lin, 1988; Zhang et al., 1991). However, few paleomagnetic data have been studied using modern instruments and data analysis techniques or methods. Lin (1988) argued that the results of Zhang and Zhang (1985) probably overprinted completely or partly by post-Proterozoic remagnetization. Lin (1988) collected 699 samples from the Paleoproterozoic Changzhougou Formation to the Neoproterozoic Jing'eryu Formation, however only over 70 samples from the Wumishan, Hongshuizhuang and Tieling Formations were regarded as reserving their primary remanences. Zhang et al. (1991) resampled over 600 samples from the same section, and 274 out of these samples covering almost the entire section from the Paleoproterozoic Changzhougou Formation to the Neoproterozoic Jing'eryu Formation were considered

Table 2

The Proterozoic paleomagnetic poles from the North China, Baltica and Laurentia blocks

Craton	Formation	D_R	I_R	$P_{lat.}$	$P_{long.}$	α_{95}	Age (Ma)	References
Laur.	Deschambault	344	68	77.0	258.0	6.0	1796 ± 15	Symons et al. (2000)
Laur.	Molson ykes	178	27	-16.0	277.0	4.0	~1750	Halls and Heaman (2000)
Laur.	St. Francois Mtn	234	9	-13.0	219.0	7.0	1476 ± 16	Meert and Stuckey (2002)
Laur.	Michikamau anorthosite	240	27	-2.0	218.0	5.0	1460 ± 5	Emslie et al. (1976)
Laur.	Harp Lake complex	253	23	2.0	206.0	4.0	1450 ± 5	Irving et al. (1977)
Laur.	Electra Lake gabbro	229	-4	-21.0	221.0	3.0	1435 ± 2	Harlan and Geissman (1998)
Laur.	Laramie anorthosite	240	16	-7.0	215.0	4.0	1429 ± 9	Harlan et al. (1994)
Laur.	Mistastin complex	256	14	-1.0	201.0	8.0	~1420	Fahrig and Jones (1976)
Laur.	Nain anorthosite	254	40	12.0	210.0	3.0	1320–1290	Emslie and Loveridge (1992)
Laur.	Mackenzie dykes	268	12	4.0	190.0	5.0	1267 ± 2	Buchan and Halls (1990)
Baltica	Ropruchey Shosksha	350	30	42.0	221.0	7.0	~1780	Pisarevsky and Sokolov (2001)
Baltica	Rödö dykes	5	30	42.0	202.0	10.0	~1513	Moakhar and Elming (1998)
Baltica	Vaasa dolerites	45	-23	7.0	164.0	4.0	1268 ± 13	Neuvonen (1966), Suominen (1991)
Baltica	Satakunta dolerites	52	-27	2.0	158.0	4.0	1264 ± 12	Neuvonen (1965), Suominen (1991)
Siberia	Kuonamka dykes	52	-25	6.0	234.0	20.0	1503 ± 5	Ernst et al. (2000)
Siberia	Chieress dykes	29	-40	4.0	258.0	7.0	1384 ± 2	Ernst et al. (2000)
NCB	North China dykes	37	-4	36.0	247.0	3.0	1769 ± 2.5	Halls et al. (2000)
NCB	Yunmengshan form.	194	-25	-60.6	87.0	3.7	~1270	Zhang et al. (2006)
NCB	Yangzhuang dolomite	98	24	2.4	190.4	11.9	~1350	This study

Abbreviations: Laur. = Laurentia; NCB = the North China Block; D_R/I_R refer to declination/inclination of a central reference location for each continent. Reference locations: Baltica: 64°N, 28°E; Laurentia: 60°N, 275°E; India: 12°N, 78°E; Siberia: 60°N, 105°E; North China: 40°N, 115°E. The rest same as Table 1.

to preserve primary remanence. Although both these two papers proposed an apparent polar wander path that was comparable with the Logan loop of Laurentia (e.g., Pesonen, 1979), the two 'Jixian loops' were assigned different age spans (1220 to ca. 1050 Ma and 1500 to ca. 1000 Ma) and their positions are over 70° apart (Li et al., 1996a, 1996b). Considering these defects, previous Proterozoic paleomagnetic results reported from the Jixian section are of very preliminary.

Paleomagnetic data from the Taihang dyke swarm is considered as a key paleopole for the North China Block at 1769.1 ± 2.5 Ma (Halls et al., 2000). The age measured by U-Pb method is of primary zircon. The mean direction for 19 dykes is $D = 36.0^\circ$, $I = -5.0^\circ$ and $\alpha_{95} = 4^\circ$ after tilt correction, yielding a paleopole at 247.0° E, 36.0° N with $dp = 2^\circ$, $dm = 4^\circ$.

Recently, Zhang et al. (2006) obtained a reliable paleopole from the Yunmengshan Formation for the North China Block (ca. 1270 Ma, Rb-Sr method), which lie at 87.0° E, 60.6° S with $\alpha_{95} = 3.7^\circ$.

Paleomagnetic data from Laurentia and Baltica have been summarized recently by Buchan et al. (2000) and Pesonen et al. (2003). Both Laurentia and Baltica possess a number of key paleopoles during ca. 1.50–1.25 Ga (Table 2). In addition, a series of less reliable data is also listed in Table 2, in order to discuss the paleoposition of these continents (Table 2). Key pole at ~1.77 Ga is not yet available from Laurentia so that its position in

this time is debated by several early attempts. For example, Halls et al. (2000) suggested that the Molson dykes pole (Halls and Heaman, 2000) is more inviting than the Deschambault Formation pole (Symons et al., 2000), in which the age of Molson dykes pole is more reliable.

In this paper, following Pesonen et al. (2003), only the low inclination case paleomagnetic data are used. The significant difference between the 1435 ± 2 Ma pole and other coeval key poles (Table 2) may be the result of unrecognized tilting of the Electra Lake gabbro during the later stages of Mesoproterozoic deformation (Harlan and Geissman, 1998) or relative motion between western North America including the Belt Basin, and the rest of Laurentia (Buchan et al., 2000). The 1320–1290 Ma pole (Murthy, 1978; Emslie and Loveridge, 1992) was obtained from the Nain anorthosite of Northeastern Laurentia, which has been used to discuss the configuration of Laurentia as a most reliable non-key paleopole (Buchan et al., 2000; Ernst et al., 2000).

The new paleopole revealed from the upper part of the Shosksha Formation at the Vazhinka River Section can be accepted as the key paleopole for Baltica at ~1.780 Ga (Pisarevsky and Sokolov, 2001). Unfortunately, there are no key paleopoles for the time interval between ca. 1.50 and 1.30 Ga from Baltica. In order to constrain the position of Baltica during the time gap, one 1513 Ma non-key pole that was evaluated and acquired as reliable pole to define the drift of Baltica is considered (Table 2).

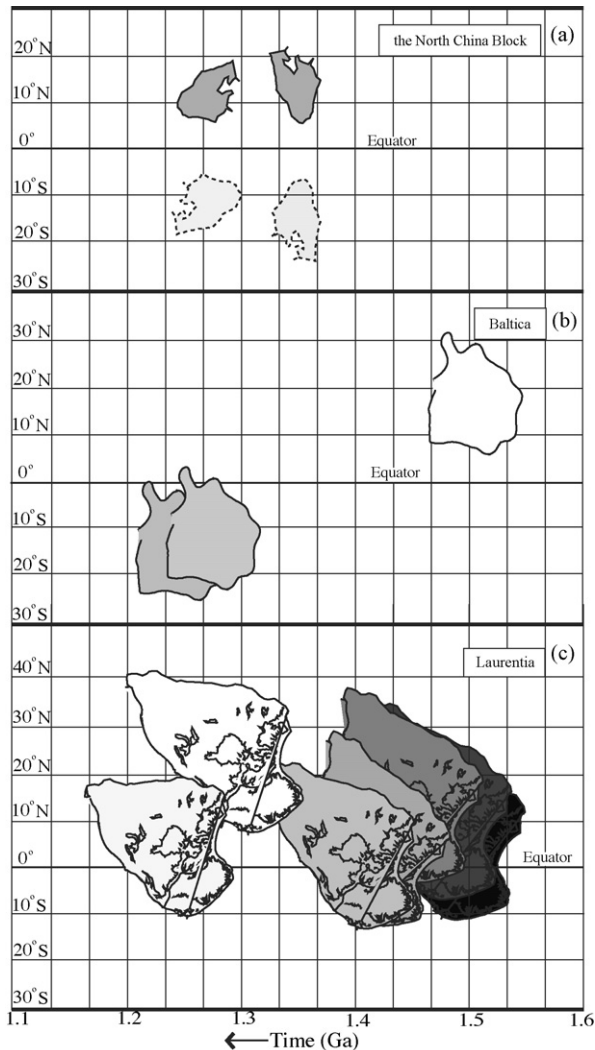


Fig. 8. Latitudinal drifts of the North China Block, Baltica and Laurentia during 1.50–1.25 Ga. (a) Paleo-latitude and orientation of the North China Block at ca. 1.35 and 1.27 Ga are based on the results from Yangzhuang Formation (this study) and Yunmengshan Formation (Zhang et al., 2006). Dashed outlines of the North China Block show other polarity locations. (b) Paleo-latitude and rotation of Baltica are based on selected non-key pole at 1.513 Ga (not shaded) and key pole at 1.268 and 1.264 Ga (shaded). (c) Positions of Laurentia are based on published non-key (not shaded) and key poles (shaded) that are discussed in the text. (b and c) only show one polarity. Actually, Baltica and Laurentia can be placed in either hemisphere because of the polarity ambiguity in the paleomagnetic data. Continents are located using GMAP for Windows computer program.

Establishing a complete Precambrian APWP is not a matter of facile task, because the time-successive poles of the craton have usually large gaps, poorly dated and polarity ambiguity. Therefore, the continents were plotted in their ancient latitudes and azimuthal orientations, which can be used for comparison of lat-

itudinal drift and rotations of the North China Block, Laurentia and Baltica between ca. 1.50 and 1.25 Ga (Fig. 8).

The Taihang dykes pole (Halls et al., 2000) suggested that Laurentia, Baltica and the North China Block may have been close to each other at 1.77 Ga in which they were spread on equatorial latitudes. The new high-quality poles from the Yangzhuang (this study) and Yunmengshan formations (Zhang et al., 2006) allow us to posit the North China Block in low latitudes between ca. 1.35 and 1.27 Ga. Although reliable poles with ages similar to that of the Yangzhuang Formation are absent from Laurentia, Baltica, there are well-dated poles for them between 1.5 and 1.25 Ga (Buchan et al., 2000; Pesonen et al., 2003; Table 2). All these poles place Laurentia, Baltica at low latitudes between 1.5 and 1.25 Ga (Fig. 8). The Yangzhuang and Yunmengshan poles also placed the North China Block in low latitudes at ca. 1.35 Ga (Fig. 8). Although the North China Block can be placed in either hemisphere with its orientation differing by 180° for ambiguity in magnetic polarity (Fig. 8). Laurentia, Baltica and the North China Block remained probably in low latitudes in this time (Buchan et al., 2000; Pesonen et al., 2003; Ernst et al., 2000). This is consistent with Laurentia, Baltica and the North China Block moving together from ca. 1.50 or 1.35 to 1.25 Ga. A recent paleomagnetic model that positions the North China Block close to Laurentia and Siberia between 1200 and 700 Ma is consistent with the proposition (Zhang et al., 2006).

5. Conclusions

This paper provides a reliable ca. 1.35 Ga paleomagnetic pole for the North China Block obtained from the Yangzhuang Formation in Jixian area of North China. The pole is considered as a key pole on the basis of positive fold test, dual polarities and lack of similarity to any known younger results. Paleomagnetic data from the ca. 1.35 Ga Yangzhuang Formation and the ca. 1.27 Ga Yunmengshan Formation place the North China Block at low latitudes during the Mesoproterozoic. Existing key poles and several most reliable poles for Laurentia and Baltica also place these continents at low latitudes between ca. 1.5 and 1.25 Ga. Thus, these data are helpful to testify the feasibility that Laurentia, Baltica and the North China Block have drifted together or close in the Mesoproterozoic.

Finally, there are some problems in the point view of the comparison of broadly coeval poles, large time gap and the polarity ambiguity. The proper reconstruction during the Mesoproterozoic requires more reliable

paleomagnetic poles with accurate ages from the North China Block and others continents.

Acknowledgments

This study was funded by the Chinese National Natural Science Foundation (40132020). Paleomagnetic data were analyzed using R. Enkin's and J.P. Cogné's computer program packets. We acknowledge Brenda Kaldenbach and two anonymous reviewers for their valuable criticism and numerous constructive improvements.

References

- Buchan, K.L., Halls, H.C., 1990. Palaeomagnetism of Proterozoic mafic dyke swarms of the Canadian Shield. In: Parker, A.J., Rickwood, P.C., Tucker, D.H. (Eds.), *Mafic Dykes and Emplacement Mechanisms*. A.A. Balkema, Rotterdam, pp. 209–230.
- Buchan, K.L., Mertanen, S., Park, R.G., Pesonen, L.J., Elming, S.A., Abrahamsen, N., Bylund, G., 2000. Comparing the drift of Laurentia and Baltica in the Proterozoic: the importance of key palaeomagnetic pole. *Tectonophysics* 319, 167–198.
- Bureau of Geology and Mineral Resources of Tianjin Municipality (BGMRT), 1989. *Regional Geology of Hebei Province, Beijing Municipality and Tianjin Municipality*. Geological Publishing House, Beijing. (in Chinese).
- Chen, J.B., Zhang, H.M., Xing, Y.S., Ma, G.G., 1981. On the Upper Precambrian (Sinian Suberathem) in China. *Precambrian Res.* 15, 207–228.
- Condie, K.C., 2002. Breakup of a Paleoproterozoic supercontinent. *Gondwana Res.* 5, 41–43.
- Emslie, R.F., Irving, E., Park, J.K., 1976. Further paleomagnetic results from the Michikamau intrusion, Labrador. *Can. J. Earth Sci.* 13, 1052–1057.
- Emslie, R.F., Loveridge, W.D., 1992. Fluorite-bearing Early and Middle Proterozoic granites, Okak Bay area, Labrador: geochronology, geochemistry and petrogenesis. *Lithos* 28, 87–109.
- Enkin, R.J., 2003. The direction-correction tilt test: an all-purpose tilt/fold test for paleomagnetic studies. *Earth Planet. Sci. Lett.* 212, 151–166.
- Ernst, R.E., Buchan, K.L., Hamilton, M.A., Okrugin, A.V., Tomshin, M.D., 2000. Integrated paleomagnetism and U–Pb geochronology of mafic dikes of the Eastern Anabar shield region, Siberia: implications for Mesoproterozoic paleolatitude of Siberia and comparison with Laurentia. *J. Geol.* 108, 381–401.
- Fahrig, W.F., Jones, D.L., 1976. The paleomagnetism of the Helikian Mistastin pluton, Labrador, Canada. *Can. J. Earth Sci.* 13, 832–837.
- Fisher, R.A., 1953. Dispersion on a sphere. *Proc. R. Soc. London, Ser. A.* 217, 295–305.
- Guan, H., Sun, M., Wilde, S.A., Zhou, X.H., Zhai, M.G., 2002. SHRIMP U–Pb zircon geochronology of the Fuping Complex: implications for formation and assembly of the North China craton. *Precambrian Res.* 113, 1–18.
- Halls, H.C., Heaman, L.M., 2000. The paleomagnetic significance of new U–Pb age data from the Molson dyke swarm, Cauchon Lake area, Manitoba. *Can. J. Earth Sci.* 37, 957–966.
- Halls, H.C., Li, J., Davis, D., Hou, G., Zhang, B., Qian, X., 2000. A precisely dated Proterozoic palaeomagnetic pole from the North China craton, and its relevance to palaeocontinental reconstruction. *Geophys. J. Int.* 143, 185–203.
- Harlan, S.S., Geissman, J.W., 1998. Paleomagnetism of the Middle Proterozoic Electra Lake Gabbro, Needle Mountains, southwestern Colorado. *J. Geophys. Res.* 103, 15497–15507.
- Harlan, S.S., Snee, L.W., Geissman, J.W., Brearley, A.J., 1994. Paleomagnetism of the Middle Proterozoic Laramie anorthosite complex and Sherman Granite, southern Laramie Range, Wyoming and Colorado. *J. Geophys. Res.* 99, 17997–18020.
- Hoffman, F.P., 1989. Speculations on Laurentia's first gigayear (2.0 to 1.0 Ga). *Geology* 17, 135–138.
- Huang, B.C., Yang, Z.Y., Zhu, R.X., 1999. Early Paleozoic paleomagnetic poles from the western part of the North China Block and their implications. *Tectonophysics* 308, 377–402.
- Irving, E., Emslie, R.F., Park, J.K., 1977. Paleomagnetism of the Harp Lake Complex and associated rocks. *Can. J. Earth Sci.* 14, 1187–1201.
- Kirschvink, J.L., 1980. The Least-Squares line and plane and analysis of paleomagnetic data. *Geophys. J. Roy. Astr. Soc.* 62, 699–718.
- Kröner, A., Wilde, S.A., Li, J.H., Wang, K.Y., 2005. Age and evolution of a late Archean to early Palaeozoic upper to lower crustal section in the Wutaishan/Hengshan/Fuping terrain of northern China. *J. Asian Earth Sci.* 24, 577–595.
- Kusky, T.M., Li, J.H., Tucker, R.D., 2001. The Archean Dongwanzi ophiolite complex, North China Craton. 2. 505-billion-year-old oceanic crust and mantle. *Science* 292, 1142–1145.
- Lee, J.S., 1939. *The Geology of China*. The Woodbridge Press, Ltd, Guilford, p. 528.
- Li, C., Peng, P.A., Sheng, G.Y., Fu, J.M., Yan, Y.Z., 2003. A molecular and isotopic geochemical study of Meso- to Neoproterozoic (1.73–0.85 Ga) sediments from the Jixian section, Yanshan Basin, North China. *Precambrian Res.* 125, 337–356.
- Li, H.K., Li, H.M., Lu, S.N., 1995. Grain zircon U–Pb ages for volcanic rocks from Tuanshanzi Formation of Changcheng System and their geological implications. *Geochimica* 24, 43–48 (in Chinese).
- Li, M.R., Wang, S.S., Qiu, J., 1996a. The ages of glauconites from Tieling and Jingeryu formations, Beijing–Tianjin area. *Acta Petrologica Sinica* 12, 416–423 (in Chinese).
- Li, Z.X., Zhang, L., Powell, C.M., 1996b. Positions of the East Asia cratons in the Neoproterozoic supercontinent Rodinia. *Austr. J. Earth Sci.* 43, 593–604.
- Lin, J.L., 1988. Middle to Late Proterozoic palaeomagnetic results from Jixian. *Chin. Sci. Bull.* 33, 207–210 (in Chinese).
- Lowrie, W., 1990. Identification of ferromagnetic minerals in a rock coercivity and unblocking temperature properties. *Geophys. Res. Lett.* 17, 159–162.
- Lu, S.N., Li, H.M., 1991. Zircon age of Dahongyu Formation. *Bull. Chin. Acad. Geol. Sci.* 22, 137–145 (in Chinese).
- Lu, S.N., Yang, C.L., Li, H.K., Li, H.M., 2002. A group of rifting events in the terminal Paleoproterozoic in the North China Craton. *Gondwana Res.* 5, 123–131.
- McElhinny, M.W., 1964. Statistics of the fold test in paleomagnetism. *Geophys. J. R. Astron. Soc.* 8, 338–340.
- McFadden, P.L., McElhinny, M.W., 1988. The combined analysis of remagnetization circle and direct observation in palaeomagnetism. *Earth Planet. Sci. Lett.* 87, 161–172.
- McFadden, P.L., McElhinny, M.W., 1990. Classification of the reversals test in palaeomagnetism. *Geophys. J. Int.* 103, 725–729.
- Meert, J.G., 2002. Paleomagnetic evidence for a Paleoproterozoic supercontinent Columbia. *Gondwana Res.* 5, 207–216.

- Meert, J.G., Stuckey, W., 2002. Revisiting the Paleomagnetism of the 1.476 Ga St. Francois Mountains Igneous Province, Missouri. *Tectonics* 21 (2), 1–19.
- Moakhar, M.O., Elming, S.-Å., 1998. Palaeomagnetic investigations of rapakivi granite complexes and associated rocks in central Sweden. In: Moakhar, M.O. (Ed.), *Rapakivi Granite and Basic Dykes in the Fennoscandian Shield: a palaeomagnetic analysis*. Ph.D. thesis. Luleå University of Technology, Luleå, Sweden.
- Murthy, G.S., 1978. Paleomagnetism results from the Nain anorthosite and their tectonic implications. *Can. J. Earth Sci.* 15, 516–525.
- Neuvonen, K.J., 1965. Palaeomagnetism of the dike systems in Finland. I. Remanent magnetization of Jotnian olivine dolerites in southwestern Finland. *CR, Geol. Soc. Finl.* 37, 153–168.
- Neuvonen, K.J., 1966. Palaeomagnetism of the dike systems in Finland. II. Remanent magnetization of dolerites in the Vaasa archipelago. *CR, Geol. Soc. Finl.* 38, 275–281.
- Pesonen, L.J., 1979. Paleomagnetism of Keweenawan igneous and baked contact rocks from Thunder Bay area, northern Lake Superior. *Bull. Geol. Soc. Finl.* 51, 27–44.
- Pesonen, L.J., Elming, S.-Å., Mertanen, S., Pisarevsky, S., D'Agrella-Filho, M.S., Meert, J.G., Schmidt, P.W., Abrahamsen, N., Bylund, G., 2003. Palaeomagnetic configuration of continents during the Proterozoic. *Tectonophysics* 375, 289–324.
- Pisarevsky, S.A., Sokolov, S.J., 2001. The magnetostratigraphy and a 1780 Ma palaeomagnetic pole from the red sandstones of Vazhinka River section, Karelia, Russia. *Geophys. J. Int.* 146, 531–538.
- Rogers, J.J.W., 1996. A history of continents in the past three billion years. *J. Geol.* 104, 91–107.
- Rogers, J.J.W., Santosh, M., 2002. Configuration of Columbia, a Mesoproterozoic Supercontinent. *Gondwana Res.* 5, 5–22.
- Suominen, V., 1991. The chronostratigraphy of southwestern Finland with special reference to Postjotnian and Subjotnian diabases. *Geol. Surv. Finl. Bull.* 356, 1–100.
- Symons, D.T.A., Symons, T.B., Lewchuck, M.T., 2000. Paleomagnetism of the Deschambault pegmatites, stillstand and hairpin at the end of the Trans-Hudson Orogen orogeny, Canada. *Phys. Chem. Earth.* 25, 479–487.
- Wang, S.S., Sang, H.Q., Qiu, J., Chen, M.E., Li, M.R., 1995. The forming ages of Yangzhuang and Wumishan formations in Jixian section, Northern China. *Scientia Geologica Sinica* 30, 166–173 (in Chinese).
- Watson, G.S., Enkin, R.J., 1993. The fold test in paleomagnetism as a parameter estimation problem. *Geophys. Res. Lett.* 20, 2135–2137.
- Wilde, S.A., Zhao, G.C., Sun, M., 2002. Development of the North China Craton during the Late Archaean and its final amalgamation at 1.8 Ga; some speculations on its position within a global Palaeoproterozoic Supercontinent. *Gondwana Res.* 5, 85–94.
- Yang, Z.Y., Ma, X.H., Huang, B.C., Sun, Z.M., Zhou, Y.X., 1998. Apparent polar wander path and tectonic movement of the North China Block in Phanerozoic. *Sci. China D41 (Suppl.)*, 51–56.
- Zhai, M.G., Liu, W.J., 2003. Paleoproterozoic tectonic history of the north China Craton: a review. *Precambrian Res.* 122, 183–199.
- Zhang, H.M., Zhang, W.Z., 1985. Palaeomagnetic data, Late Precambrian magnetostratigraphy and tectonic evolution of Eastern China. *Precambrian Res.* 29, 65–75.
- Zhang, H.M., Zhang, W.Z., Elston, D.P., 1991. Palaeomagnetic study on Middle and Late Proterozoic rock in Jixian, North China. *Acta Geophysica Sinica* 34, 602–615 (in Chinese).
- Zhang, S.H., Li, Z.X., Wu, H.C., 2006. New Precambrian palaeomagnetic constraints on the position of the North China Block in Rodinia. *Precambrian Res.* 144, 213–238.
- Zhao, G.C., Cawood, P.A., Wilde, S.A., Sun, M., 2002. Review of global 2.1–1.8 Ga orogens: implications for a pre-Rodinia supercontinent. *Earth Sci. Rev.* 59, 125–162.
- Zhao, G.C., Sun, M., Wilde, S.A., 2003. Correlations between the Eastern Block of the North China Craton and the South Indian Block of the Indian Shield: an Archean to Paleoproterozoic link. *Precambrian Res.* 122, 201–233.
- Zhao, G.C., Sun, M., Wilde, S.A., Li, S.Z., 2004. A Paleo-Mesoproterozoic supercontinent: assembly, growth and breakup. *Earth Sci. Rev.* 67, 91–123.
- Zhao, G.C., Sun, M., Wilde, S.A., Li, S.Z., 2005a. Late Archean to Paleoproterozoic evolution of the North China Craton: key issues revisited. *Precambrian Res.* 136, 177–202.
- Zhao, Y., Song, B., Zhang, S.H., Ma, Y.S., Pei, J.L., Yang, Z.Y., 2005b. New U-Pb SHRIMP constraints on the age of Late Triassic deformation in Yanshan Fold Belt. In: *Beijing SHRIMP center annual report (Abstract Volume)*. Geological Publishing House, Beijing. (in Chinese).